

1 Supplement to “Volcanic Spreading and Lateral Variations in the Structure of Olympus  
2 Mons, Mars”, by P. J. McGovern and J. K. Morgan.

3

4 **Method.**

5 We use Particle Dynamics models (PD, also known as Distinct Element Method, or  
6 DEM) to calculate the deformation of a large volcanic edifice subject to variations in  
7 basal slope and friction. The procedure used in our numerical experiments follows that of  
8 Morgan and McGovern (2005), and is described below, with the most pertinent boundary  
9 conditions described in the main text. The PD code TRUBAL resolves contact forces  
10 acting on discrete particles, and solves Newton’s equations of motion for each particle to  
11 maintain quasi-static equilibrium of the assemblage. Volcanic edifice growth is simulated  
12 by “raining” frictional particles on a planar substrate. Once each increment of particles  
13 has settled, particle positions, contacts, and forces are recorded for processing. The  
14 simulations used 9600 particles, deposited in increments of 300, to yield high-resolution  
15 models. Note that in general, the left sides of the models are intended to correspond to the  
16 northwest flank of Olympus Mons, and the right sides to the southeast flank.

17 At the summit of Olympus Mons, a zone of very low slope (also broadest to the  
18 southeast and south) encompasses the caldera complex. When the effects of caldera faults  
19 are filtered out, the entire summit constitutes a broad low-slope region (Fig. 2). This  
20 flatness indicates an inability to sustain broad-scale slopes over mechanically weak  
21 magma chambers. To reflect this, in some models we assign the lowest values of basal  
22 friction  $\mu_b$  to a small basal patch near the center of the edifice, to reflect the inability of a  
23 fluid-filled magma chamber to support broad-scale slopes above it. Without it, some

24 models develop “pointy”, high-sloped summits that do not resemble the broad, flat  
25 Olympus Mons summit region. This patch is not meant to represent the basal friction in  
26 this region *per se*.

27 Lateral variations in internal friction are not considered here; effective internal  
28 friction is fixed at  $\sim 0.6$ . While we do not explicitly model the effects of lithospheric  
29 flexure on basal slopes, models with outward-decreasing friction may mimic several slip-  
30 inhibiting effects of flexure, including outward flux of pore fluid (due to gradients in  
31 lithostatic pressure (McGovern and Solomon, 1997) and temperature) and inward-  
32 increasing basal slopes.

### 33 **Figures.**

34 Supplementary Figure DR1. Topography cross-sections and broad-scale slopes derived  
35 from MOLA topography for four profiles through the caldera of Olympus Mons. Half-  
36 profiles are defined by azimuth from the caldera center ( $18.35^\circ$  N,  $226.8^\circ$  E). Left vertical  
37 axis: black line denotes topography in km; data interval 500 m; vertical exaggeration  
38 approximately 7:1. Right vertical axis: diamond symbols denote magnitudes of along-  
39 track slopes derived from a least-squares-fit line to an 80-km-wide flank segment  
40 centered on the x-coordinate of the symbol. Slopes with magnitudes greater than 12  
41 degrees are plotted at the 12-degree value. (a) NW-SE profile (azimuths 315 and 135). (b)  
42 NW-SE profile (azimuths 300 and 120). (c) NE-SW profile (azimuths 45 and 225). (d)  
43 NE-SW profile (azimuths 60 and 240).

44 Supplementary Figure DR2. Filtered broad-scale slopes of a NW-SE-oriented section of  
45 Olympus Mons (corresponding to that in Figure 2 of the main text), calculated from  
46 MOLA  $1/128^{\text{th}}$  degree topography. Solid line indicates  $\pm 300$  km from center of caldera

47 complex oriented along  $135^\circ$  and  $315^\circ$  azimuths. Broad-scale slopes are calculated by a  
48 least-squares planar fit to topography points within an 80-km diameter circle. This figure  
49 provides a direct comparison to the slope plots of Figure 3 and Supplementary Figure 3 in  
50 terms of the baseline distance (80 km) over which slopes are calculated.

51

52 Supplementary Figure DR3. Evolution of edifice slopes as functions of load increment for  
53 four DEM models of volcanic spreading. Bottom plot: edifice slopes for each load  
54 increment, filtered by averaging over 80 km-wide bins; the absolute value of slope is  
55 shown. Edifice bases are marked by black curves. Top plot: basal friction as a function of  
56 distance. (a) Model M2 (constant friction, no basal slope), to address point raised in first  
57 paragraph of “results” section regarding wedge-like deformation and convex morphology  
58 being characteristic of constant friction models, regardless of slope. (b) Model M23,  
59 outward-decreasing friction with superposed 0.6 degree basal slope, to illustrate point  
60 raised in second paragraph of “Results” section that basal slope has only a slight effect on  
61 the nature of deformation on the uphill flank. (c) Model M20, leftward-decreasing  
62 friction with superposed 0.6 degree basal slope, to illustrate point raised in third  
63 paragraph of the “Discussion” section that basal slope has only a slight effect on the  
64 convex shape of the uphill flank.

65

66 Supplementary Figure DR4. Stratigraphy and internal deformation of the same DEM models  
67 of volcanic spreading shown in Figure 3. Top plot: Color-coded stratigraphy denoted by  
68 green, gold, and white layers. Each color layer constitutes four 300-element load  
69 increments. Bottom plot: Horizontal displacement gradient field: red denotes horizontal

70 extension, blue denotes horizontal contraction. Strain magnitude is denoted by color

71 intensity. (a-c) correspond to same models shown in Supplementary Figure 3.

72

73

74

75 **Movies:**

76

77 Supplementary Movie 1: Surface topography, stratigraphy, and horizontal displacement  
78 gradient field for model M8: constant friction with  $0.6^\circ$  basal slope (the model in Figures  
79 3a and 4a-b). Note: movies use TRUBAL code coordinates, which are in .1 meter  
80 increments.

81

82 Supplementary Movie 2: Same as above for model M23: friction decreasing outward  
83 from center, no basal slope (the model in Figures 3b and 4c-d).

84

85 Supplementary Movie 3: Same as above for model M18: friction decreasing to left, no  
86 basal slope (the model in Figures 3b and 4e-f).

87

88 Supplementary Movie 4: Same as above for model M31: friction decreasing to left,  $0.3^\circ$   
89 basal slope (the model in Figures 3b and 4g-h).

90

91

Figure DR1

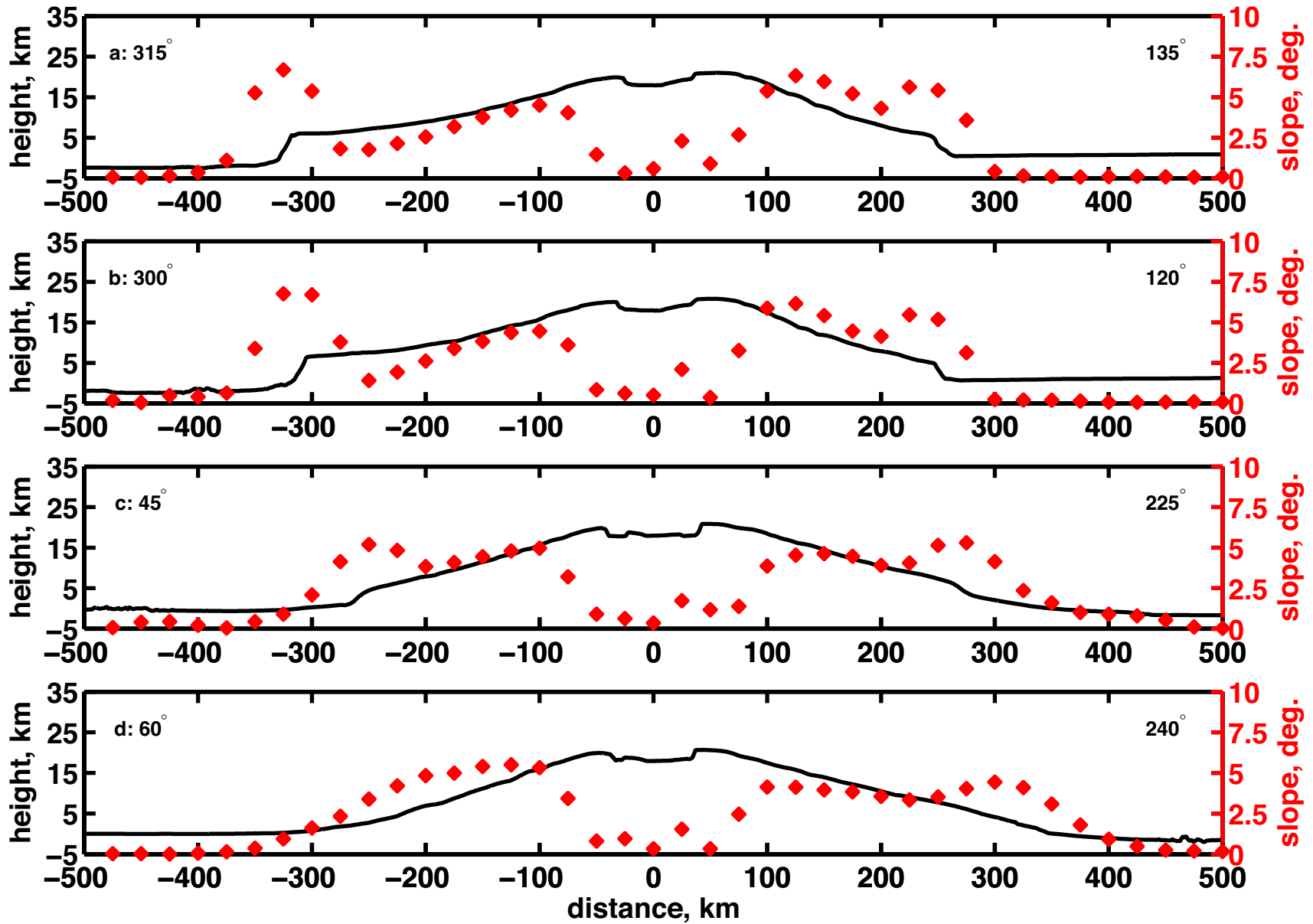


Figure DR2

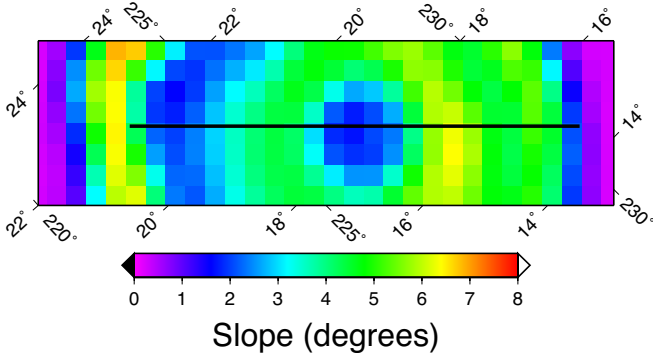


Figure DR3

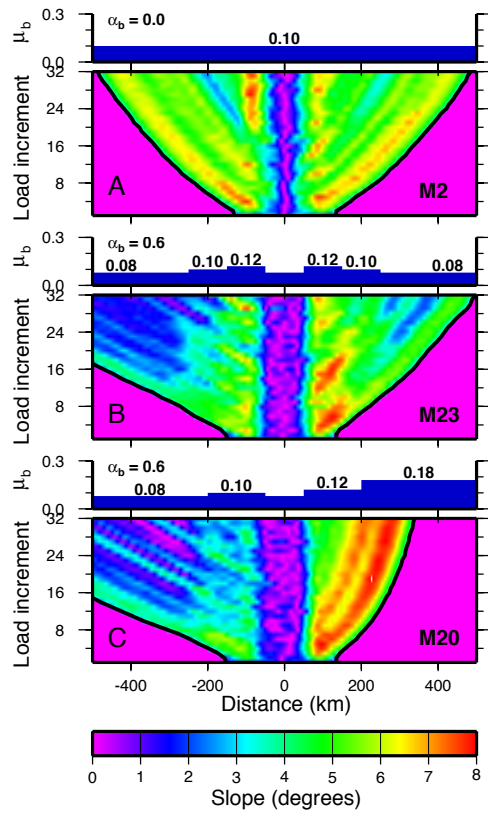


Figure DR4

